Available online at www.sciencedirect.com

ScienceDirect

Energy Procedia 1 (2009) 845–852

Physics Procedia

www.elsevier.com/locate/procedia

Pressure Drop and Mass Transfer of a High Capacity Random Packing. Application to CO_2 Post-combustion Capture.

Pascal ALIX[a], Ludovic RAYNAL

IFP, Rond Point de l'Echangeur 69360 Solaize, FRANCE

Abstract

Pressure drop and interfacial area have been measured for a modern high capacity random packing. Pressure drop and flooding limit are found to be in good agreement with the manufacturer software. It is observed that the interfacial area, a_e, is linked to the flooding percentage and can be much higher than the geometric area. However a_e depends slightly on the chemical system, this can be explained by gas limitation. The selected packing seems to be well adapted for CO_2 capture process, since pressure drop is low and interfacial area is high. Present results have been used successfully to model the CASTOR pilot plant for post-combustion CO_2 capture.

effective area; pressure drop; random packing ; CO2 capture ; reactive absorption

doi:10.1016/j.egypro.2009.01.112

1. Introduction

To reduce greenhouse gases emissions, the E.U. CASTOR[1] project target is to enable the capture and geological storage of the CO_2 emitted by power plants. Huge gas flowrates must be treated for post-combustion capture of CO_2, which leads to very large capture amines plants. The optimisation of such high volume reactor design is thus of great importance. This calls for the development of reliable models for pressure drop and mass transfer characteristics determination.

Since capture process operates downstream the power plant, it requires very low pressure drop. For the absorber, the overall pressure drop, including the inlet and the outlet of the column, should be lower than 100 mbar. To meet these requirements of size optimisation and pressure drop limitation, efficient high capacity packings are needed. In the framework of CASTOR project, two recent high capacity packings have been considered for chemical engineering studies [1]. To build-up models, tests are highly needed to characterize these packings in terms of hydrodynamic and mass transfer. The aim of the present study is to determine the pressure drop and the interfacial area for one of the two selected packings : the IMTP50 random packing. Since one assumes that MEA 30%wt is the base case for the process [2;3], one can consider that fast reactions will occur in capture plants. The interfacial area, a_e, becomes the main parameter to estimate the efficiency of an absorber [4].

In the following, experimental set-ups and methods are first described. Second, results are shown and discussed. Last data are given in order to model the pilot plant.

2. Methods and materials

2.1. Columns and packed beds geometries

Experiments have been carried out in three columns ; first a 150 mm internal diameter column with a bed height of 1.7 meter, second a 400 mm internal diameter column for with a bed height of 1.5 meter, last the CASTOR pilot plant itself. It consists in a 1100 mm internal diameter column, and is equipped with four packed beds, for each bed the height being equal to 4.25 meter.

The two first columns operate at atmospheric pressure and room temperature. Gas is air or nitrogen and liquid is water. Liquid load, Q_L, varies from 10 to 120 $m^3/m^2/h$. Superficial gas velocity, V_{SG}, varies from 0 to 2 m/s which leads to a F-Factor, $F_S = \sqrt{\rho_G} \times V_{SG}$, varying from 0 to 2.4 $Pa^{0.5}$ where ρ_G is the gas density. The drip point density of the liquid distributor, *dp*, which is the number of liquid injectors by surface area, is close to 680 m^{-2}. According to Fair and Bravo [5], Aroonwilas *et al.* [6] and Alix and Raynal [1], it is high enough to ensure that the distributor does not influence the results.

For the CASTOR pilot plant, the pressure is close to the atmospheric pressure and the temperature varies from 40 to 70°C. Gas is flue gas and solvent is MEA 30%wt or CASTOR 2. Table 1 gives the liquid viscosity, μ_L, and the surface tension, σ, for the different solvents. Q_L varies from 10 to 40 $m^3/m^2/h$, F_s varies from 0 to 2 $Pa^{0.5}$. *dp* is close to 100 m^{-2}, it is high enough to ensure that the distributor does not influence the results strongly [1].

Table 1: Fluid properties.

Fluid	T (K)	μ_L (Pa.s)	σ (dyne/cm)
Water	303	0.8	71
MEA 30%wt	323	1.2	56
CASTOR 2	323	3.8	35

[1] www.co2-castor.com

Figures 1a and 1b give a picture of single elements and packed bed of IMTP50 respectively. Geometric characteristics of the packed beds are given in Table 2. One can observe that the bed density is lower for the 150 mm diameter column, while the values obtained with the 400 mm diameter column and the pilot plant are similar to each other and close to the one given for industrial plants [7]. Despite a lower density, the geometric area is not reduced for the 150 mm diameter since column walls are taken into account. However this indicates that a scale effect could appear for the smaller column.

a/

b/

Figure 1 : Single elements and packed bed of IMTP50.

Table 2 : Geometric characteristics of the IMTP50.

Column Inner Diameter, d (mm)	150	400	1100
Single element of packing : Width, Proof (mm)	20 ; 40		
Packed Bed Void Fraction, ε (%)	98		
Packed Bed Density, ρ_{bed} (kg/m^3)	130	156	159
Calculated Geometric Specific Area, a_g (m^2/m^3)	110		
State of surface, Material	smooth, 316L		

2.2. Pressure drop measurements

Pressure drop is measured with two inclined or horizontal tubes. It has been checked that, if one uses the same pressure tap geometry for both sampling ports, this geometry does not influence results. However this geometry is critical to prevent any accumulation of liquid in transducer lines with gas-liquid flows. It has to be noticed that the lines of the transducer are purged before each measurement. For wetted conditions pressure drop fluctuates in time, present values are thus time averaged over a period of 2 minutes. Pressure drop is measured between the inlet and the outlet of the bed but for the pilot plant. For the latter, pressure drop cumulates the packed bed and the corresponding liquid distributor. In all cases, relative error is estimated between 10 and 20%.

2.3. Effective area measurements

In the present study, three CO_2/NaOH systems have been chosen : NaOH at 1N with air as used by [8], NaOH at 0.1N with air as used by [9], NaOH at 1N with air and added CO_2 (up to 2% vol, [10]). A pseudo-first order reaction, a fast reaction regime and a negligible gas side resistance are assumed. This leads to [4] :

$$\phi_{CO2} = \frac{E.k_L}{He}.P_{CO2}.a_e = \frac{\sqrt{D_{CO2}.k_2.C_{OH}^{\ 0}}}{He}.P_{CO2}.a_e \qquad (1)$$

ϕ_{CO2} is the absorption rate of CO_2 . E, is the enhancement factor and takes into account the effect of the chemical reaction on ϕ_{CO2}. k_L is the liquid side mass transfer coefficient. P_{CO2}, is the partial pressure of CO_2. Kinetic constant, k_2, CO_2 liquid diffusion coefficient, D_{CO2}, and Henry constant, He, have been calculated with relations given by Pohorecki and Moniuk [11].

Within the packed column, one dimensional and stationary plug flows of liquid and gas are assumed. The column is assumed to be isotherm and isobar. The CO_2 gas molar fraction is measured at the inlet and at the outlet of the column via gas chromatography or infra-red. From previous studies on liquid distribution [1], liquid flow is considered homogeneous. Then the effective area, a_e, is assumed to be constant. From the inlet CO_2 molar fraction, $y_{CO2,in}$, a_e is the only parameter to adjust in order to fit the CO_2 outlet molar fraction. Then the CO_2 profile directly gives a_e. Liquid samples are taken at the inlet and outlet of the column. CO_3^{2-} and OH^- amounts are measured by HCl titration. Then, the concentration of OH^- in the liquid bulk, $C_{OH}^{\ 0}$, is known at the column inlet and outlet, and can be implemented into the 1D model. Mass balance between the gas and the liquid phase has thus been checked.

3. Results and discussion

3.1. Pressure drop

Figure 2 gives the packed bed dry pressure drop for the three columns as a function of F_s. First, it appears that results are very different with the 150 mm diameter column in terms of absolute values and slope. This indicates that there is a scale effect between 150 and 400 mm diameter columns. This was expected since the bed density is lower at 150 mm (Table2), and this is in agreement with Henriques de Brito *et al*. [12] since the ratio between d and the dimensions of a packing element (Table 2) is lower than 8 at 150 mm. At 150 mm, the slope of the curve equals 0.8 which is comparable to a gas laminar flow in pipes. At 400 and 1100 mm, the slope of the curve equals 1.9 which is first comparable with a turbulent gas flow in pipes, and second in agreement with the manufacturer software (KG-Tower 3.2) and literature [8;13]. At 400 mm diameter, pressure drop is well predicted by KG-Tower 3.2. However, the pressure drop in the CASTOR pilot is 30% higher.

Figure 3 gives the packed bed wetted pressure drop for the 400 mm diameter column for two liquid loads. It appears that KG-Tower 3.2 predicts well the pressure drop, the loading point and the flooding point. Figure 4 gives the wetted pressure drop for the 400 mm diameter column and the pilot plant, for Q_L=20 $m^3/m^2/h$.. For the latter, operating range in terms of gas and liquid flowrates is not large enough to reach the loading point, however two solvents have been used (Table 1). First it appears that fluid properties don't modify the pressure drop below the loading point which is in agreement with KG-Tower 3.2. Second, the pilot plant pressure drop is again 30% higher than the predicted one. This could be explained by at least two reasons :

- some gypsum is entrained by the flue gas from the FGD plant and is deposited on packing elements, which modifies the void fraction then increases the pressure drop,
- the liquid distributor gives a higher pressure drop than the estimated one.

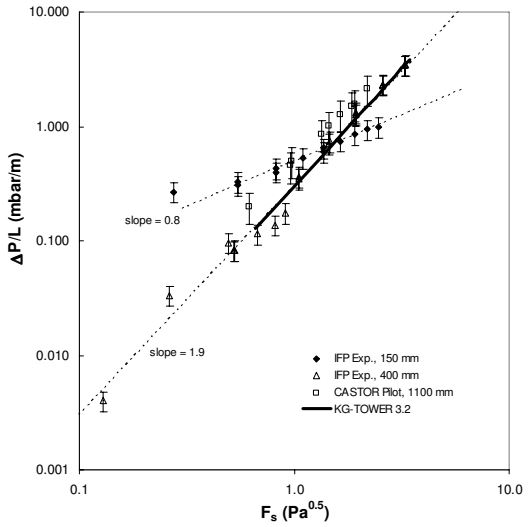

Figure 2 : Dry pressure drop as a function of F_s. Comparison with KG-Tower 3.2 software.

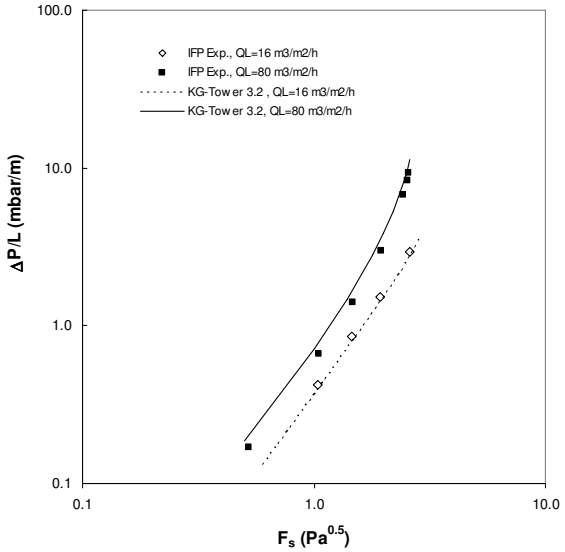

Figure 3 : Wetted pressure drop for the 400 mm diameter column as a function of F_s. Comparison with KG-Tower 3.2 software.

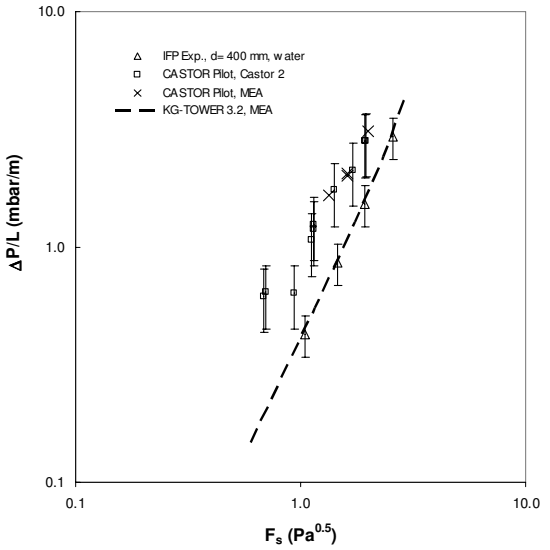

Figure 4 : Wetted pressure drop for the pilot plant as a function of F_s for two solvents and Q_L=20 $m^3/m^2/h$. Comparison with KG-Tower 3.2 software and present results obtained with the 400 mm diameter column.

3.2. Effective area

Figure 5 gives the ratio of the effective to the geometric area as a function of the flooding percentage, F_c, mesured with different chemical systems. F_c is the ratio between F_s and the F-Factor at the flooding point for the same liquid load, $F_{s,fl}$. The latter can be calculated by KG-Tower 3.2 (cf. 3.1). The effective area is calculated via relation (1). For all chemical systems, E is higher than 5 and much lower than the instantaneous enhancement factor, E_i, since ratio E_i/E is higher than 40 for all cases and all systems. This tends to valid fast reaction regime and pseudo first order reaction, and indicates that these systems should lead to similar results.

One observes that, for the same chemical system, results obtained at 150 mm are different from those obtained at 400 mm, in terms of absolute values and slope of the curve. This was expected since a scale effect is observed for pressure drop.

At 400 mm, a_e is systematically 10% higher with the air-0.1N than the one measured with the air-1N system. This last result was not expected. Relation (1) assumes that ϕ_{CO2} is not limited by the mass transfer from the gas to the liquid. If one considers gas resistance, a general expression of ϕ_{CO2} can be given by relation (2) with k_G being the gas side mass transfer coefficient. Relation (2) shows that, if ($1/k_G$) is not negligible compared to ($He/E.k_L$), ϕ_{CO2} is reduced which leads to decrease the calculated a_e if the model does not take into account k_G effect. Then, a gas limitation can explain differences between the two previous systems since the ratio between ($1/k_G$) and ($He/E.k_L$) is minimum for the 0.1N-air system.

$$\phi_{CO2} = \left(\frac{1}{k_G} + \frac{He}{E.k_L} \right)^{-1} .a_e.P_{CO2} \qquad (2)$$

a_e is systematically 10% higher for air-1N than the one measured with air+CO_2-1N. The latter can not be explained by a gas side limitation since ratios between ($1/k_G$) and ($He/E.k_L$) are similar. It has to be noticed that the instantaneous enhancement factor, E_i, is inversely proportional to the CO_2 partial pressure [4]. Then E_i is much lower for air+CO_2-1N than the one for air-1N. Differences between these two systems could be explained by the fact that the pseudo first reaction assumption is not fully valid for air+CO_2-1N system. This was not expected since E is, as previously discussed, in the good range.

Last, Figure 5 shows that a_e can be 50% higher than a_g. This can be explained by rivulets and droplets formation, which is in agreement with Alix and Raynal [1]. This is an interesting result since a_e should be maximum for the present process. For different structured packings, Seibert et al. [9] show that effective areas tend to reach the geometric ones but are always lower. Then, random and structured packings should not be compared in terms of geometric area only. For the CASTOR pilot plant, CO_2 profiles and temperature have been measured with MEA 30%wt and F_c close to 60%. From figure 5 it is possible to give a very simple and accurate correlation to estimate a_e and model the pilot.

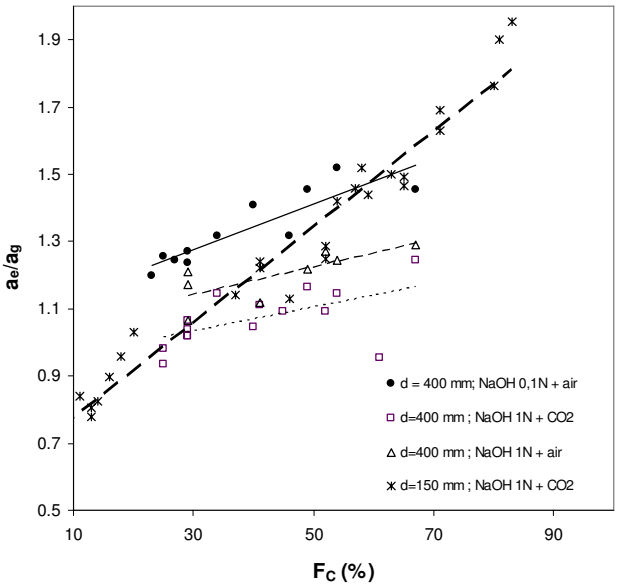

Figure 5 : Ratio of the effective and the reference area as given by relation (1) as a function of F_c, for different chemical systems and inner diameters.

Relation (2) is equivalent to :

$$\begin{cases} \dfrac{P_{CO2}}{\phi_{CO2}} = \dfrac{1}{k_G.a_e} + \dfrac{He}{E.k_L.a_e} = \dfrac{1}{k_G.a_e} + \dfrac{He}{\sqrt{k_2.D_{CO2}.C_{OH^-}^{0}}.a_e} \\ \Leftrightarrow Y = \dfrac{1}{k_G.a_e} + \dfrac{1}{a_e} \times X \end{cases} \qquad (3)$$

Relation (3) corresponds to a Danckwerts plot [4], the intercept of the linear fit gives $k_G.a_e$, the slope gives a_e. With present experiments, X parameter is very different for 0.1N and 1N solutions. For one fixed operating conditions in terms of gas and liquid flows, it is possible to draw the corresponding Danckwerts plot (Figure 6). The slope of the curve gives an interfacial area which is very similar to the one obtained with 0.1N-air system. The corresponding k_G equals 9.10^{-6} mol/m^2/Pa/s. It is in agreement with correlations proposed by Onda [14] or Fair and Bravo [5] for similar packings. This tends to show that gas limitation is negligible with air-0.1N system but must be taken into account for other systems.

If one assumes that a_e is given by 0.1N-air system, k_G can be estimated from air-1N experiments by using relation (3) instead of (1) in the model. k_G varies from 5.10^{-6} to 2.10^{-5} mol/m^2/Pa/s while V_{sG} ranges between 1 and 2 m/s.

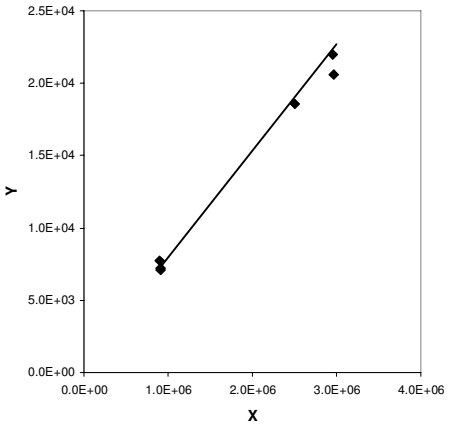

Figure 6 : Danckwerts plot for F_c=29 %.

4. Conclusions

To reduce the size of future post-combustion capture plants, high capacity and low pressure drop packings are highly needed and must be fully characterized for further use in process simulators. In this study, the IMTP50 random packing has been tested. Pressure drop and interfacial area have been measured over a large range of operating conditions. A scale effect is observed between 150 mm and 400 mm diameter columns. Below the loading point, pressure drop is not sensitive to fluid properties. The manufacturer software can thus be used to estimate both pressure drop and flooding limit. Surprisingly, the pilot plant gives very high pressure drop. This can be explained by gypsum deposit or liquid distributor effect.

It is observed that for this metallic random packing the interfacial area is much higher than the geometric one. a_e is proportional to the flooding percentage which leads to very simple correlations. It is observed that a_e depends slightly on the chemical system if no gas limitation is assumed. To reduce this effect, the air-0.1N system is recommended. Present packing seems to be well adapted for post-combustion capture plants, since it generates low pressure drop and high interfacial area. Present results will be used to model the pilot plant with MEA [15].

5. References

1. P. Alix, L. Raynal. Chem. Res. Design 86(6), (2008) 585-591.
2. J.N. Knudsen, P.J. Vilhelmsen, JN Jensen, O. Biede, VGB Conference, Chemie im Kraftwerk, 11-12 Oct., Germany (2006).
3. P.H.M. Feron, M. Abu-Zahra, P. Alix, O. Biede, P. Broutin, H. de Jong, J. Kittel, J. Knudsen, L. Raynal, P.J. Vilhelmsen, *3th International Conference on Clean Coal Technologies for our Futur, Cagliari, Italy (2007).*
4. P.V. Danckwerts, McGraw-Hill : New-York (1970).
5. J.R. Fair, J.L. Bravo, Chemical Engineering Progress, 86(1), (1990) 19-29.
6. A. Aroonwilas, P. Tontiwachwuthikul, A. Chakma, Separation and Purification Technology, 24, (2001) 403-411.
7. IMTP Brochure, Bulletin KGIMTP-I 2M0303B (2003).
8. M. Duss, H. Meierhofer, E. Dale, Chem. Eng. Technol, 24(7), (2001) 716-723.
9. F. Seibert, I. Wilson, C. Lewis, G. Rochelle, Greenhouse Gas Control Technol., II, (2005) 1925-1928.
10. L. Raynal, J.P. Ballaguet, C. Barrere-Tricca, Chemical Engineering Science, 59, (2004) 5395-5402.
11. R. Pohorecki, W. Moniuk, Chem. Engineering. Science, 43(7), (1988) 1677-1684
12. M. Henriques de Brito, U. von Stockar, A. Menendez Bangerter, P. Bomio, M. Laso, Ind. Eng. Chem. Res, 33 (1994) 647-656.
13. L. Speigel, W. Meier, IchemE Symposium Series No.128, (1992) B85-B94.
14. K. Onda, H. Takeuchi, Y. Okumoto, Journal of Chemical Eng. of Japan, 1(1), (1968) 56-62.
15. R. Dugas, GHGT-9 presentation

The authors would like to thank the European Commission for its financial support under the CASTOR project.